Synthesis of Vinyl–Trivinyl Acidic Resins for Application in Catalysis: Statistical Study and Site Accessibility Assessment

William M. Godoy [1] , Leandro G. Aguiar [1,]*, Nuno A. B. S. Graça [2] and Alírio E. Rodrigues [2]

1 Department of Chemical Engineering, Engineering School of Lorena, University of São Paulo, Lorena 12602-810, SP, Brazil
2 LSRE-LCM, Associate Laboratory ALiCE, Department of Chemical Engineering, Faculty of Engineering, University of Porto (FEUP), 4200-465 Porto, Portugal
* Correspondence: leandroaguiar@usp.br

Abstract: This study aimed to synthesize sulfonated polymer resins based on styrene and trimethylolpropane triacrylate (TMPTA) and evaluate their catalytic efficiency in glycerol acetylation. A factorial design was used, with two factors, three levels, and three replicates of the center point. The factors were cross-linker percentage (Y_{TMPTA}) and cross-linker feed time (T_{TMPTA}). Ion-exchange capacity, swelling index, and catalytic efficiency were analyzed to characterize each resin. Lower cross-linker percentages resulted in higher catalytic efficiencies, as expected. Resins synthesized with 2, 6, and 10% TMPTA had mean catalytic efficiencies of 215, 176, and 121, respectively. A linear correlation was observed between catalytic efficiency and cross-linker percentage, with $R^2 = 0.9971$. Statistical and kinetic models were developed to represent the experimental results and support the development of strategies to improve resin formulation and synthesis conditions. TMPTA feed time at low and high levels positively influenced catalytic efficiency; the result is attributed to the micro- and macrostructure of resins. This finding was corroborated by the kinetic constants provided by the model.

Keywords: acetylation; catalyst; glycerol; resin; styrene

1. Introduction

Recent studies have developed polymer resins for application in water treatment [1], chemical catalysis [2], and biocatalysis [3]. In the last decades, ion-exchange resins have been used as catalysts in different organic reactions [4]. Such resins consist mainly of cross-linked sulfonated polymers produced by styrene–divinylbenzene copolymerization and can be applied to increase the rate of etherification [5], esterification [6], acetylation [7], and acetalization [8]. Studies by Amberlyst [9], Dowex [10], Purolite [11], and Lewatit [12] have applied commercially available resins in the aforementioned reactions. Favorable characteristics of these materials include high adsorption capacity for different adsorbents, ranging from highly hydrophobic to highly hydrophilic species, structures that are conducive to the formation of catalytic sites, high specific surface area, high swelling and ion-exchange capacities [13,14] and easy separation and recycling [15]. Polystyrene cross-linked with divinylbenzene is the most used resin. It has an outstanding ion-exchange capacity (ranging from 0.8 to 5.6 mmol g^{-1}) and is available in different crosslinking and sulfonation degrees [11]. Nonetheless, recent studies have shown that commercial styrene–divinylbenzene resins may contain inaccessible catalytic sites owing to hindering effects in specific regions of the material [4]. According to the literature, resins with low divinylbenzene percentages are more flexible, leading to a favorable morphology for catalytic applications [16], as this allows for a greater number of catalytic sites to be accessible to the reaction medium. Studies have investigated the use of other cross-linkers to overcome hindering effects, such as ethylene glycol dimethacrylate (EGDMA) [17] and triethylene glycol dimethacrylate (TEGDMA) [18]. This strategy explores the effects of chain length

variation, as divinylbenzene is a cross-linker with a relatively small chain length [19]. This study used an experimental design to investigate the influence of trimethylolpropane triacrylate (TMPTA) as a cross-linker and the effect of cross-linking density on resin catalytic efficiency. A statistical study was conducted to identify the optimum conditions for the synthesis of styrene–TMPTA catalysts in the studied ranges. This goal was achieved by analyzing the catalytic efficiency of synthesized resins in glycerol acetylation. Additionally, a kinetic model was developed to assess catalytic site accessibility and its effect on the rate constant of each reaction step.

2. Results and Discussion

The results of the study are divided into the following subsections: (i) Catalyst Synthesis and Characterization, which presents a discussion on catalyst properties; (ii) Catalytic Tests, which describes the study of catalytic efficiency based on statistical analyses; and (iii) Kinetic Model and Site Accessibility Assessment, which focuses on kinetic behavior and accessibility characteristics of polymer resins.

2.1. Catalyst Synthesis and Characterization

Experiments were performed according to a factorial design with triplicate runs of the center point, as described in Section 3.1. Experimental conditions and their respective polymerization and sulfonation yields are presented in Table 1.

Table 1. Experimental conditions and polymerization (PY) and sulfonation (SY) yields.

Run	Factor		Response	
	Y_{TMPTA}	T_{TMPTA}	PY (%)	SY (%)
1	0.10	30	77	89
2	0.10	150	85	82
3	0.10	270	88	82
4	0.06	30	73	85
5	0.06	150	90	93
6	0.06	270	92	80
7	0.02	30	73	83
8	0.02	150	74	82
9	0.02	270	57	73
10	0.06	150	93	91
11	0.06	150	100	93

Y_{TMPTA}, cross-linker content; T_{TMPTA}, cross-linker feed time. A two-phase feed program was used. From 0 to 30 min of reaction, TMPTA was fed into the reactor at 10 min intervals. From 30 min onward, TMPTA was fed at 20 min intervals. In all cases, the total amount of cross-linker was divided into equal portions throughout the reaction.

Polymerization yields were satisfactorily compared with those of a previous study using the same comonomer system [20]. Sulfonation results show low mass loss (about 15%), which is expected for styrene–acrylate systems [17]. After the sulfonation reaction, all resins were characterized for ion-exchange capacity. Swelling indices were calculated at the end of glycerol acetylation, as described in the Methods section. Results are presented in Table 2.

Ion-exchange capacity was similar among resins, and was about $0.5 \, \text{mmol g}^{-1}$, which is considerably lower than the values of most commercial resins (4.0–$5.4 \, \text{mmol g}^{-1}$). These differences may be explained by the relatively mild sulfonation conditions (short reaction time and low temperature) used in the current study to avoid crossing the degradation threshold of styrene–acrylate-based resins [17]. Sulfonation conditions were not varied in this work. Further studies are needed to investigate the sulfonation limits of styrene–TMPTA resins and enhance their ion-exchange capacity.

Table 2. Properties of sulfonated resins.

Resin	Y_{TMPTA}	T_{TMPTA} (min)	IEC (mmol g^{-1})	S_w
S1	0.10	30	0.585	1.177
S2	0.10	150	0.540	1.344
S3	0.10	270	0.540	1.463
S4	0.06	30	0.418	1.214
S5	0.06	150	0.641	1.440
S6	0.06	270	0.537	1.355
S7	0.02	30	0.357	1.244
S8	0.02	150	0.413	1.104
S9	0.02	270	0.411	1.578

Y_{TMPTA}, cross-linker content; T_{TMPTA}, cross-linker feed time; IEC, ion-exchange capacity; S_w, swelling index. Results for S5 are the mean values of three resins obtained under center point conditions (runs 5, 10, and 11).

The swelling index indicates the degree to which resins are able to swell and change morphology. Table 2 shows that, on average, the swelling index did not change considerably as a function of TMPTA content in the acetylation medium, despite the higher chain density of resins produced with higher cross-linker percentages (2 to 10%). Swelling ability also depends on the affinity between resin and the medium [21]. Based on the functional groups involved in the present catalytic process, it can be stated that resin polarity becomes more similar to the polarity of the acetylation medium as acrylate (TMPTA) content increases. Thus, competing effects (cross-linking density versus resin–medium affinity) may explain why the swelling index remained practically constant as TMPTA content increased. On the other hand, mean swelling indices increased slightly as TMPTA feed time increased from 30 to 270 min. This finding suggests that a better distribution of monomer units along copolymer chains can improve the swelling index and potentially provide higher accessibility to catalytic sites.

After the characterization step, all resins were subjected to catalytic tests for performance assessment. The catalytic efficiency of each resin was calculated from glycerol consumption (or acetate production) and ion-exchange capacity, as described in the next section.

2.2. Catalytic Tests

Glycerol acetylation was carried out under the same conditions for all resins (acetic acid/glycerol molar ratio of 4:1, 90 °C, and 40 g L^{-1} catalyst). Results are presented in Table 3.

Table 3. Glycerol conversion (X_G) and catalytic efficiency (E_f) of polymer resins.

Resin	Y_{TMPTA}	T_{TMPTA} (min)	IEC (mmol g^{-1})	X_G (%)	E_f
S1	0.10	30	0.585	86	98
S2	0.10	150	0.540	66	90
S3	0.10	270	0.540	63	87
S4	0.06	30	0.418	78	173
S5	0.06	150	0.641	72	83
S6	0.06	270	0.537	88	181
S7	0.02	30	0.357	64	147
S8	0.02	150	0.413	34	84
S9	0.02	270	0.411	90	206

Y_{TMPTA}, cross-linker content; T_{TMPTA}, cross-linker feed time; IEC, ion-exchange capacity. Conversions and efficiencies calculated from glycerol content at 1 h of reaction.

It can be observed from Table 3 that glycerol conversion at 1 h of reaction is similar between S6 and S9 (about 90%), indicating better catalytic performance when the cross-linker is well distributed along the polymer matrix (TMPTA feed time of 270 min). However, it is also necessary to consider catalytic efficiency. Catalytic efficiency results show the

behavior of each catalyst in relation to its ion-exchange capacity. Results are expressed in mol of glycerol consumed per mol of catalytic site at 1 h of reaction.

Runs S1 to S3, which were conducted using 10% cross-linker in the polymer matrix, resulted in lower catalytic efficiency than runs S7 to S9, whose cross-linker content was 2%. These findings suggest a considerable influence of cross-linker concentration on catalytic efficiency, with catalytic efficiency decreasing as the polymer matrix becomes denser (higher cross-linker content). In spite of the coherence of the aforementioned results, it is understood that each resin has its particular swelling kinetics. At the beginning of the catalytic process, it is not likely that all accessible catalytic sites are available, as the swelling process is still ongoing. Therefore, in order to assess the efficiency of fully swollen resins, mean catalytic efficiency (E_{fE}) of resins was calculated at 6 h of reaction for each TMPTA content (2% TMPTA, runs 7–9; 6% TMPTA, runs 4–6; and 10% TMPTA, runs 1–3). The results are shown in Figure 1.
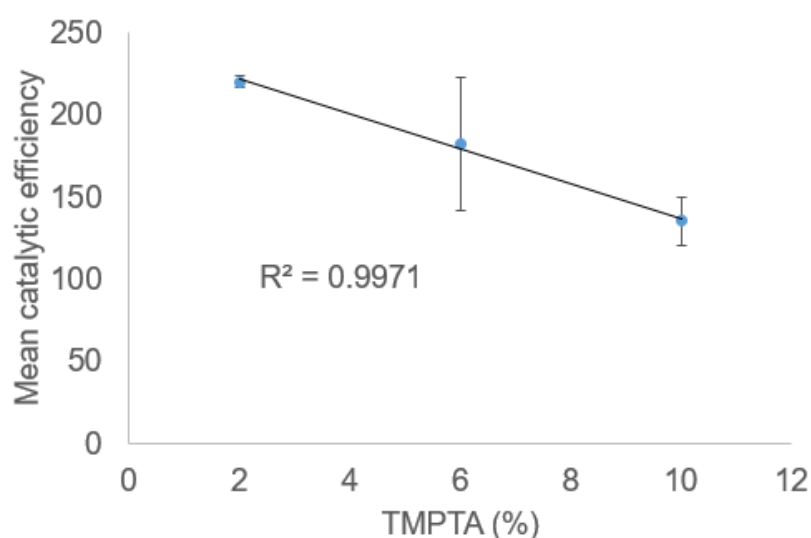

Figure 1. Mean catalytic efficiency calculated from glycerol consumption at 6 h of reaction for resins prepared with different TMPTA contents.

Figure 1 shows that there is an almost linear decreasing trend of catalytic efficiency with increasing TMPTA content, which was expected because tighter polymer networks are formed with higher TMPTA contents, reducing accessibility to catalytic sites. The large standard deviation bars are justifiable, as they were determined with data from different experiments.

To statistically corroborate the relationship between catalytic efficiency and cross-linking density, the effects of Y_{TMPTA} and T_{TMPTA} factor levels on the signal-to-noise ratio was assessed using an analysis of variance (Figure 2) [22].

Figure 2 shows the relationship between signal-to-noise ratio and Y_{TMPTA} and T_{TMPTA} levels. For Y_{TMPTA}, there was an increase in signal-to-noise ratio with decreasing cross-linker percentage and was significant at levels two and three. On the other hand, for T_{TMPTA}, the highest ratios were observed at levels one and three. At 10% cross-linker (level one), the ratio was significant, becoming non-significant at 6% (level two) and returning to a significant point at 2% (level three). This behavior can be explained by the occurrence of competing effects, which will be discussed in the Kinetic Model and Accessibility Assessment Section 2.3.
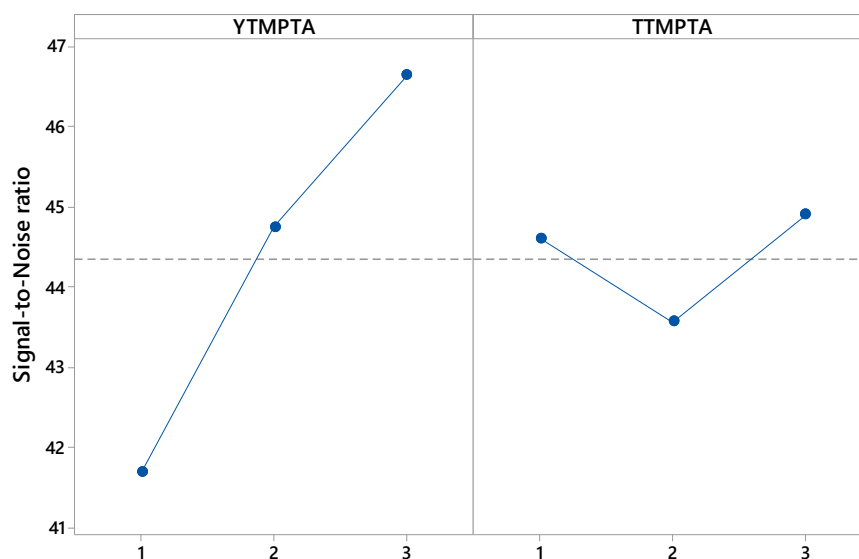
Figure 2. Effect of factors on signal-to-noise ratio. The dashed line represents the significance threshold.

In summary, based on the results of the evaluated effects, it was found that low cross-linker percentage has a significant effect on catalytic efficiency. This finding is corroborated by the calculated *F*-value ($F = 9.18$), which is higher than the critical *F* statistic ($F = 6.94$) [23]. On the other hand, cross-linker feed time was not a significant factor according to *F*-statistics, but it was relevant or close to significant, according to Phadke (1983) [24], because high and low factor levels were above the significance threshold (Figure 2), demonstrating a positive influence on the final result.

A statistical model was developed to identify which synthesis conditions provide the best catalytic efficiency (Equation (1)). The equation was obtained through a multiple regression analysis (minimizing the sum of squared errors) using the solver tool from LibreOffice®.

$$E_f = 109.99 + 87.87 \times Y_{TMPTA} - 85.12 \times T_{TMPTA} - 4.03 \times Y_{TMPTA} \times T_{TMPTA}$$
$$-8.31 \times Y_{TMPTA}^2 + 23.65 \times T_{TMPTA}^2 \tag{1}$$

The statistical model was fitted to experimental data with an R^2 of 0.85. According to the model, the optimum experimental conditions in the studied range are Y_{TMPTA} and T_{TMPTA} at level three (2% cross-linker fed over 270 min in the copolymerization step), which provided a catalytic efficiency of 220 at 6 h of reaction. This result was expected, given that a lower cross-linker percentage, as discussed earlier, increases the flexibility of polymer chains, facilitating the flow of compounds (reagents and products) in the reaction medium.

2.3. Kinetic Model and Accessibility Assessment

Comparisons between model predictions and experimental data were carried out for catalytic efficiency as a function of reaction times of interest (i.e., reaction times where there was high consumption or production of a given compound). For glycerol and triacetin, this comparison was made at $t = 6$ h, whereas for monoacetin and diacetin, the reaction time was $t = 2$ h. The results are illustrated in Figure 3.
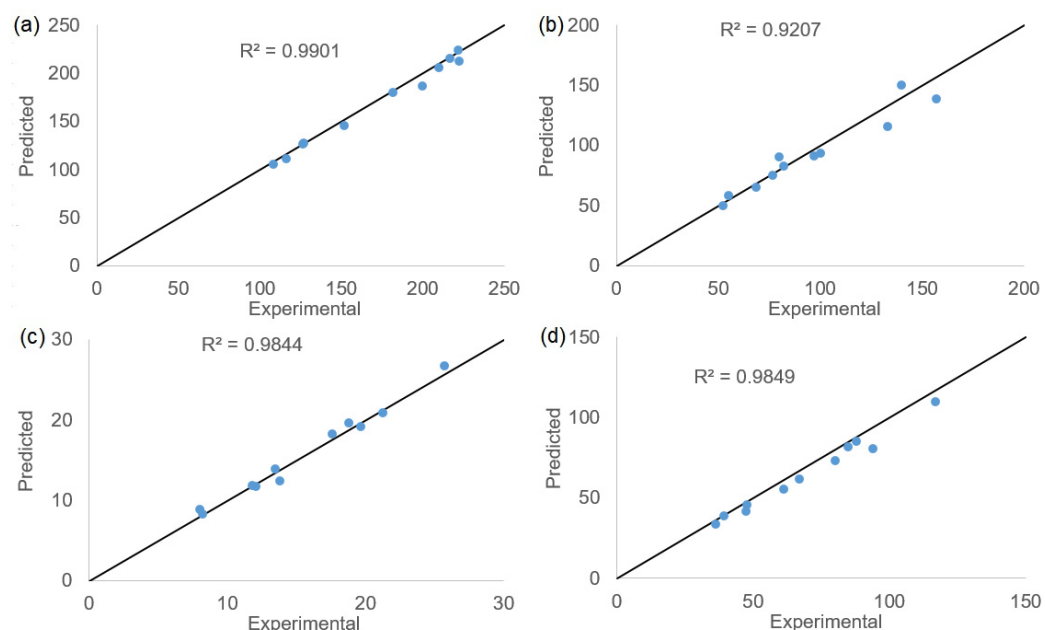
Figure 3. Comparison of experimental versus predicted catalytic efficiencies. (**a**) Catalytic efficiencies calculated from glycerol consumption at 6 h of reaction. (**b**) Catalytic efficiencies calculated from monoacetin production at 2 h of reaction. (**c**) Catalytic efficiencies calculated from diacetin production at 2 h of reaction. (**d**) Catalytic efficiencies calculated from triacetin production at 6 h of reaction.

The models' fittings provided R^2 values in the range of 0.92 to 0.99, indicating good predictive ability. Similar model fits were obtained with other concentration profiles. Figure 4 shows the curve fitting for the optimum conditions identified by statistical analysis ($Y_{TMPTA} = 0.02$, $T_{TMPTA} = 270$ min). Fitted parameters are presented in Table 4.
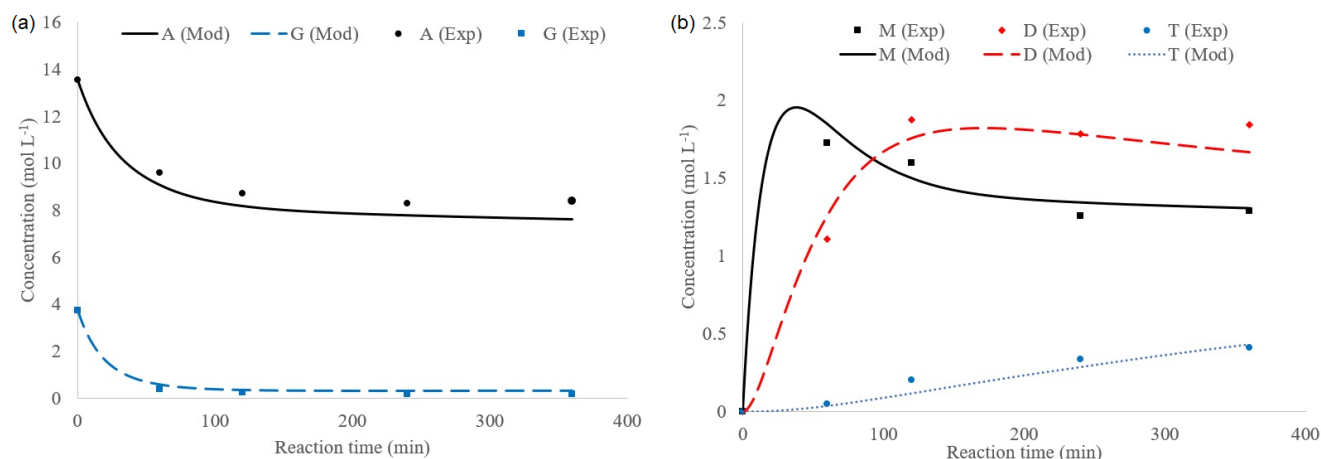

Figure 4. Curve fitting for concentration profiles of run S9 ($Y_{TMPTA} = 0.02$, $T_{TMPTA} = 270$ min). Exp—experimental data; Mod—kinetic model predictions; (**a**) Glycerol and acetic acid concentrations: A—acetic acid; G—glycerol; (**b**) Acetates concentration: M—monoacetin; D—diacetin; T—triacetin.

Table 4. Model parameters.

Run	Resin Formulation		k_1 $(L^2\ mol^{-2}\ min^{-1})$	k_2 $(L^2\ mol^{-2}\ min^{-1})$	k_3 $(L^2\ mol^{-2}\ min^{-1})$
	TMPTA Content (%)	TMPTA Feed Time (min)			
S1	10	30	0.1100	0.0550	0.0041
S2	10	150	0.0800	0.0210	0.0030
S3	10	270	0.0650	0.0150	0.0022
S4	6	30	0.1500	0.0390	0.0045
S5	6	150	0.1240	0.0380	0.0034
S6	6	270	0.1000	0.0570	0.0048
S7	2	30	0.1200	0.0270	0.0031
S8	2	150	0.0760	0.0180	0.0039
S9	2	270	0.2100	0.0890	0.0061

TMPTA, trimethylolpropane triacrylate. Parameters fitted for all cases: K_{eq1} = 3, K_{eq2} = 1, and K_{eq3} = 0.7. $k_1^0 = 1.67 \times 10^{-4}$, $k_2^0 = 5.50 \times 10^{-5}$, $k_1^0 = 7.00 \times 10^{-7}$ L mol^{-1} min^{-1}.

The effects of TMPTA feed time on catalytic efficiency and the kinetic parameters of the model are presented in Figure 5. Mean k_i values were calculated from data presented in Table 4.
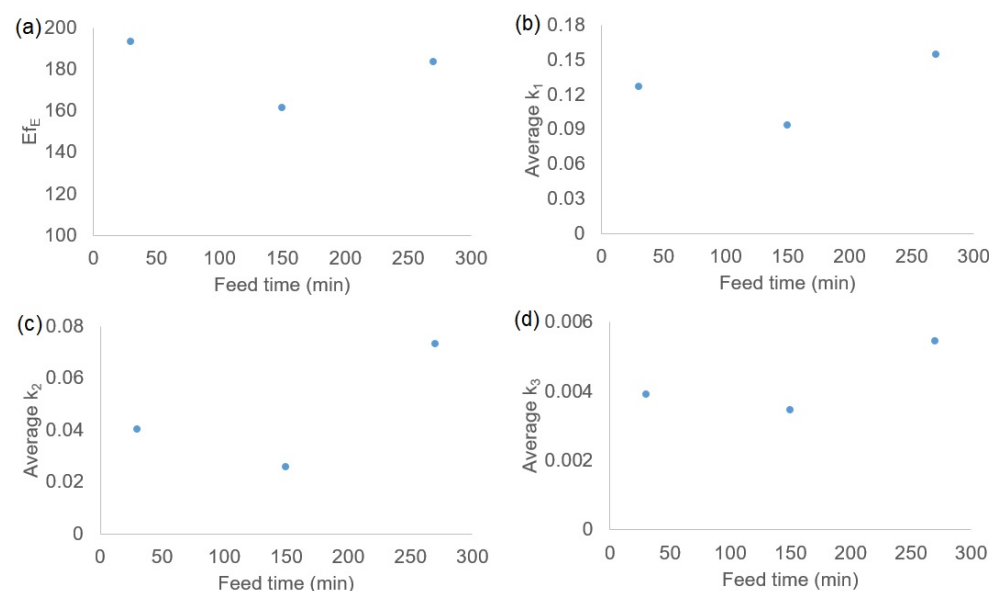
Figure 5. Effect of TMPTA feed time on catalytic efficiency (E_{fE}) and kinetic parameters (k_1, k_2, k_3). (**a**) Average experimental catalytic efficiency of glycerol consumption in 6 h of reaction ($L^2\ mol^{-2}\ min^{-1}$). Average rate constants of reactions: (**b**) 1, (**c**) 2, and (**d**) 3.

In Figure 5, means were calculated for runs 1, 4, and 7 (feed time = 30 min), 2, 5, and 8 (feed time = 150 min), and 3, 6, and 9 (feed time = 270 min).

Different from that suggested in Figure 1, the molecular structure was not the factor predominantly affected by TMPTA feed time. The formation of meso- and macropores is favored when the cross-linker concentration is increased during copolymerization [25]. Thus, when the cross-linker (TMPTA) is fed in a more concentrated manner (e.g., its total mass is fed in only 30 min), the catalytic efficiency and rate constants are relatively high because of the attractive macroporous structure. On the other hand, when the same cross-linker mass is distributed over a long period of copolymerization (e.g., 270 min), the accessibility of molecules to the resulting microstructure seems to be favored, also resulting in high values of E_{fE} and k_i. Therefore, the variation in TMPTA feed rate has opposite effects on resin molecular structure and macrostructure, leading to low accessibility in the case of intermediate cross-linker distribution (150 min), as depicted in Figure 5.

The fraction of accessible catalytic sites (f_{ASi}) was assessed relative to the highest k_i values, which were obtained for run S9 (k_1 = 0.21, k_2 = 0.089, k_3 = 0.0061 $L^2\ mol^{-2}\ min^{-1}$).

Maximum accessibility was assumed for S9, i.e., $f_{AS1} = f_{AS2} = f_{AS3} = 1$, resulting in $k_1^S = 0.21$, $k_2^S = 0.089$, and $k_3^S = 0.0061$ L^2 mol^{-2} min^{-1}. Given that k_1^S, k_2^S, and k_3^S refer to reactions on catalytic sites, regardless of the chain architecture of each resin, the values are the same for S1 to S9. These values were used to calculate the f_{ASi} of all resins by using data from Table 4 and Equation (13). Accessibility data were compiled into mean f_{AS} values, resulting in $f_{AS} = 0.62$ for resins with 2% TMPTA, $f_{AS} = 0.60$ for resins with 6% TMPTA, and $f_{AS} = 0.42$ for resins with 10% TMPTA. To establish a correlation with concepts of accessibility from the literature, we assumed factor f_{AS} to be the Ogston coefficient (K_O) for a molecule whose diameter (d_m) corresponds to the average diameter of all species involved in the reaction. With this, it was possible to estimate the average chain density for the resins synthesized here, as depicted in Equation (2) [11,26]:

$$C = -\frac{\ln(K_O)}{0.25\pi(d_m + d_c)^2} \tag{2}$$

where C is the chain density, K_O is the Ogston coefficient, d_c is the diameter of polymer chain rigid rods ($d_c = 0.4$ nm) [11], and d_m is the molecule diameter. In the current study, d_m was considered to be equal to 0.65 nm, the average of estimated molecular diameters of acetic acid, glycerol, monoacetin, diacetin, triacetin, and water [27]. Figure 6 shows the mean chain densities (C) of styrene–TMPTA resins, as calculated by using Equation (2), and a comparison with chain densities of commercial resins [28].
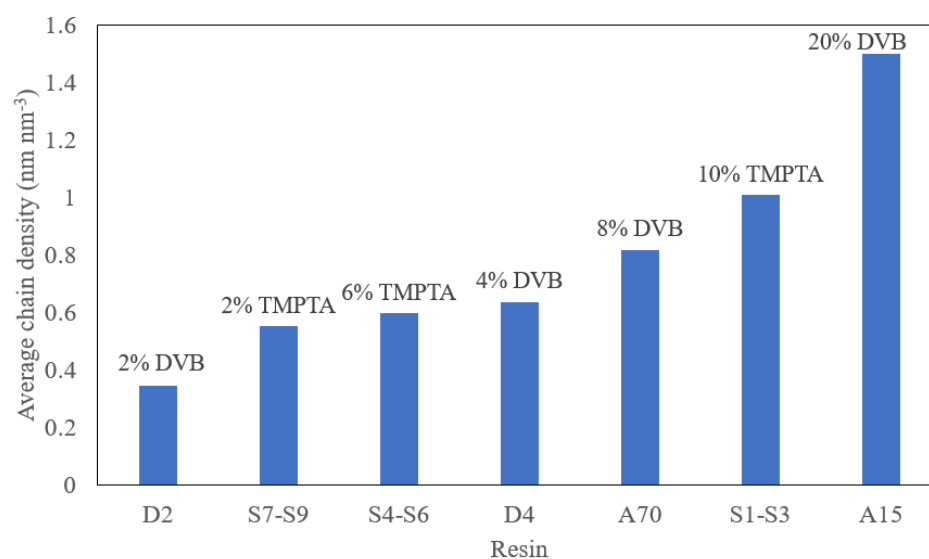
Figure 6. Mean chain densities of commercial and synthesized resins. D and A represent the commercial resins Dowex and Amberlyst, respectively [28].

TMPTA is a trivinyl cross-linker; thus, each cross-linking point can form up to six chains, whereas the limit of divinylbenzene is four chains. On the other hand, the chain density near cross-linking points is attenuated because of the resulting homogeneity of TMPTA feed time and its long chain branches as compared with divinylbenzene. In view of these compensating features of TMPTA, it was expected that the resins produced here would not be significantly displaced in the chain density scale in comparison with divinylbenzene. This expectation was confirmed by the results of Figure 6.

3. Methods

3.1. Factorial Design

Styrene–TMPTA resins were formulated according to a factorial design. A 3^2 factorial arrangement with two center points was used to investigate factor effects [29]. The factors were cross-linker molar fraction in relation to monomers (Y_{TMPTA}) and TMPTA feed time (T_{TMPTA}) at three levels, as shown in Table 5.

Table 5. Factorial design.

Level	Factors	
	Y_{TMPTA}	T_{TMPTA} (min)
1	0.10	30
2	0.06	150
3	0.02	270

The matrix containing all experimental conditions is presented in the Results and Discussion section.

3.2. Suspension Copolymerization

Suspension copolymerization for the synthesis of the catalyst support was carried out according to a procedure described in the literature [7,30], with modifications. The cross-linker was fed at specific reaction times. Suspension copolymerization was performed in a 1 L jacketed glass reactor at 80 °C and 350 rpm for 6 h. The reactor was fed with a mixture of organic (11.5 vol%) and aqueous (88.5 vol%) phases. The aqueous phase consisted of a solution of polyvinyl alcohol (0.0038% *w/v*) in water. The solution was purged with nitrogen gas (15 mL min^{-1}) for 1 h, and then the organic phase was fed into the reactor. The organic phase consisted of a mixture of 1 mol% benzoyl peroxide (initiator) relative to the monomer mixture (styrene + TMPTA), different fractions of TMPTA in the monomer mixture (0.02, 0.06 and 0.10), 30 vol% monomers in the organic phase, and 50% toluene in the solvent mixture (toluene + heptane). The cross-linker (TMPTA) was fed into the reactor at pre-defined times, according to Table 5.

After each run, the polymerization yield was calculated by dividing the amount of polymer produced by the amount of monomers fed into the reactor.

3.3. Sulfonation Reaction

Resin sulfonation was carried out according to the literature [7,31]. About 10 g of dried resin was added with concentrated sulfuric acid (140 mL) at 57 °C under stirring (175 rpm) for 1 h. Subsequently, the mixture (resin + sulfuric acid) was diluted in distilled water at 25 °C and filtered. The sulfonated resin was extensively washed to remove all residual acid and oven-dried at 50 °C to constant weight. The sulfonation yield was calculated by dividing the mass of sulfonated resin by the mass of resin measured at the beginning of the sulfonation reaction (10 g) [7].

### 3.4. Ion-Exchange Capacity

Ion-exchange capacity was determined according to a method described elsewhere [32]. About 0.5 g of dried sulfonated resin was mixed with 8 mL of nitric acid solution (1 mol L^{-1}) for 4 h. Subsequently, resins were filtered and dried at 50 °C until constant weight was achieved. The dried resin was immersed in 30 mL of sodium hydroxide solution (0.1 mol L^{-1}) and left to rest for 24 h. The resulting solution was titrated with hydrochloric acid (0.1 mol L^{-1}), and ion-exchange capacity was estimated according to Equation (3):

$$IEC = \frac{C_{NaOH} \times V_{NaOH} - C_{HCl} \times V_t}{W_d} \qquad (3)$$

where IEC is the ion-exchange capacity (mmol g^{-1}), C_{HCl} is the concentration of hydrochloric acid (mmol mL^{-1}), C_{NaOH} is the concentration of sodium hydroxide solution, V_{NaOH} is the volume of sodium hydroxide solution (mL), V_t is the titrated volume of hydrochloric acid (mL) and W_d is the resin dry weight (g).

3.5. Glycerol Acetylation

Glycerol acetylation was performed to test the catalysts. Operating conditions were based on previous studies [33,34]. The acetic acid/glycerol molar ratio was 4:1, the catalyst concentration was 40 g L^{-1}, and the reaction was conducted at 90 °C under magnetic stirring for 6 h. At pre-set times, aliquots were withdrawn from the reactor and analyzed using a Shimadzu Nexis GC-2030 gas chromatograph equipped with a SH-Rtx-5 column and a flame ionization detector for quantification of all species. Acetic acid concentration was also determined by acid–base titration. Figure 7 illustrates the set of reactions involved in glycerol acetylation.
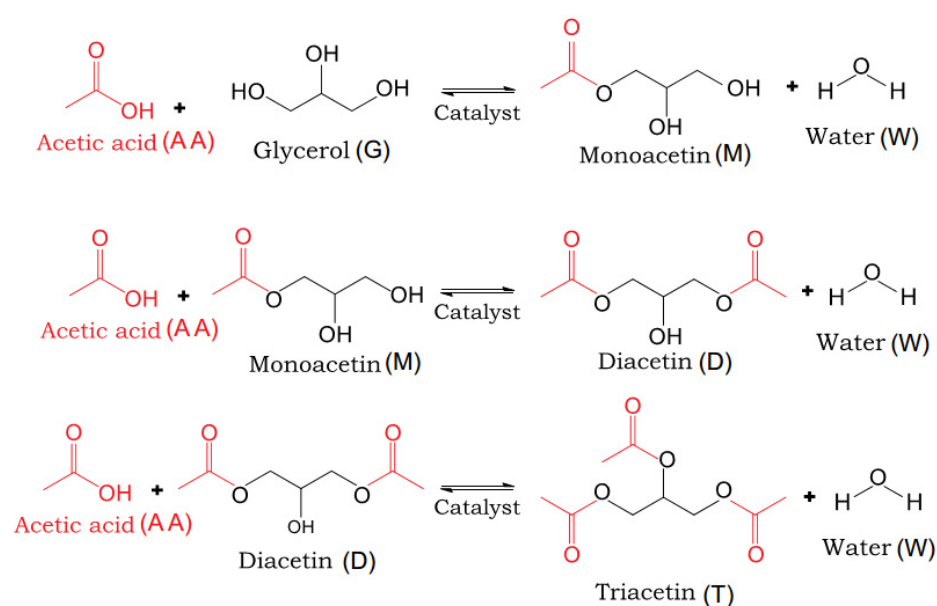
Figure 7. Glycerol acetylation. The isomers 1- and 2-monoacetin and 1,2- and 1,3-diacetin are formed during the process [35].

3.6. Swelling Index

After the glycerol acetylation reaction, resins were filtered, weighed (W_{SW}), and dried to constant weight (W_d). The swelling index (S_w) was calculated as shown in Equation (4).

$$S_w = \frac{W_{SW}}{W_d} \qquad (4)$$

3.7. Catalytic Efficiency

In this study, the catalytic efficiency of each resin was calculated as the number of mols consumed/produced per mol of catalytic site at a given time, as described in Equation (5) [7]:

$$E_f = \frac{N_c}{\text{IEC} \times M_{cat}} \qquad (5)$$

where E_f is the catalytic efficiency, N_c is the number of mols of glycerol consumed (or of acetate produced) at the end of the reaction (mol), IEC is the ion-exchange capacity (mol g^{-1}) and M_{cat} is the amount of resin fed to the reactor (g).

3.8. Kinetic Modeling

A kinetic model was developed for the glycerol acetylation reaction catalyzed by the synthesized acidic resins. The reactions illustrated in Figure 7 can be expressed by chemical Equations (6) to (8), and the respective rate equations are listed in Equations (9) to (11).

$$\text{Reaction 1}: \ \text{AA} + \text{G} \rightleftarrows \text{M} + \text{W} \tag{6}$$

$$\text{Reaction 2}: \ \text{AA} + \text{M} \rightleftarrows \text{D} + \text{W} \tag{7}$$

$$\text{Reaction 3}: \ \text{AA} + \text{D} \rightleftarrows \text{T} + \text{W} \tag{8}$$

$$r_1 = \left(k_1^0 + k_1^S f_{AS1} C_{cat} \text{IEC}\right)\left[C_{AA} C_G - \frac{C_M C_W}{K_{eq1}}\right] \tag{9}$$

$$r_2 = \left(k_2^0 + k_2^S f_{AS2} C_{cat} \text{IEC}\right)\left[C_{AA} C_M - \frac{C_D C_W}{K_{eq2}}\right] \tag{10}$$

$$r_3 = \left(k_3^0 + k_3^S f_{AS3} C_{cat} \text{IEC}\right)\left[C_{AA} C_D - \frac{C_T C_W}{K_{eq3}}\right] \tag{11}$$

where r_i is the rate of reaction i (mol L^{-1} min^{-1}), k_i^0 is the rate constant of the uncatalyzed reaction i (mol L^{-1} min^{-1}), k_i^S is the rate constant of the catalyzed reaction i (L^2 mol^{-2} min^{-1}), f_{ASi} is the fraction of catalytic sites accessible to compounds of reaction i, C_{cat} is the catalyst concentration (g L^{-1}), IEC is the ion-exchange capacity of the resin (mol g^{-1}), K_{eqi} is the equilibrium constant of reaction i and C_j is the concentration of species j (mol L^{-1}).

The rate constant k_i was defined as follows (Equation (12)):

$$k_i = k_i^S f_{ASi}, \ i = 1, \ 2, \ 3 \tag{12}$$

In Equation (12), k_i^S and f_{ASi} were grouped so that the resulting parameter, k_i, contains information of accessibility to resin catalytic sites. It is known that a detailed assessment of resin site accessibility can be carried out by analyzing properties such as chain density distribution (via inverse size exclusion chromatography) and Ogston coefficient for each compound [16,28]. Nonetheless, a simplified approach was used here, assuming an average fraction of catalytic sites accessible to the compounds of reaction i (f_{ASi}).

Molar balances are described in Equations (13) to (18).

$$\frac{dC_G}{dt} = -r_1 \tag{13}$$

$$\frac{dC_M}{dt} = r_1 - r_2 \tag{14}$$

$$\frac{dC_D}{dt} = r_2 - r_3 \tag{15}$$

$$\frac{dC_T}{dt} = r_3 \tag{16}$$

$$\frac{dC_{AA}}{dt} = -r_1 - r_2 - r_3 \tag{17}$$

$$\frac{dC_W}{dt} = r_1 + r_2 + r_3 \tag{18}$$

Differential equations were solved numerically in Scilab by adjusting a set of uncatalyzed reaction rate constants (k_1^0, k_2^0, k_3^0) and equilibrium constants (K_{eq1}, K_{eq2}, K_{eq3}) for all cases and a set of catalyzed reaction rate constants (k_1, k_2, k_3) for each resin. The R^2 values for glycerol, acetic acid, monoacetin, diacetin, and triacetin curve fittings were calculated. The best fit was achieved by adjusting the set of parameters that provided the maximum mean R^2 for each resin.

Despite the acidic nature of the styrene–TMPTA resins developed here, stemming from the presence of sulfonic groups, the polarity of the matrix is much more pronounced than that of styrene–divinylbenzene resins. Given this prominent difference, the adsorption/desorption equilibrium parameters of glycerol acetylation on styrene–divinylbenzene resins reported in the literature were not adopted in this work. In order to avoid overfitting, the adsorption/desorption kinetics were not considered for the resin, resulting in a reduced number of parameters (simplified model).

Strictly speaking, the rate equations should be written in terms of compound activities. However, as reactions were carried out at atmospheric pressure, the activities can be replaced by concentrations, as described in Equations (9) to (11).

The objective of the modeling part of this research was to estimate the rate constants for the different resin formulations at the set temperature. This made it possible to discuss the accessibility of compounds to the catalytic sites of each resin. The kinetic data obtained here can be a starting point for further studies to determine the Arrhenius equation parameters by conducting experiments under different temperature conditions.

4. Conclusions

Acidic styrene–TMPTA resins were synthesized using different cross-linker contents and feed times and tested as catalysts in glycerol acetylation. A factorial design was carried out, and the optimum resin formulation was found to be that which contained 2% TMPTA fed along the first 270 min of copolymerization, according to a statistical equation. The mean catalytic efficiency decreased markedly with increasing TMPTA content, demonstrating the effect of reduced accessibility in dense polymer networks. The mean swelling index did not vary significantly with TMPTA content; however, it showed a slight increase with increasing TMPTA feed times. A kinetic model was constructed and validated with experimental data, providing R^2 values of about 0.97. The average rate constants of all reactions had a behavior that indicates competing effects (resin macrostructure versus microstructure), in which lower values correspond to the intermediate TMPTA feed time (150 min). This finding is corroborated by the catalytic efficiency profile, which behaved similarly as a function of the TMPTA feed time. TMPTA can be copolymerized with styrene and be sulfonated. Despite the low ion-exchange capacities produced under the sulfonation conditions studied here, styrene–TMPTA resins show attractive accessibility when applied as catalysts.

Author Contributions: Conceptualization, N.A.B.S.G.; methodology, W.M.G. and L.G.A.; formal analysis, A.E.R.; writing—original draft preparation, W.M.G.; writing—review and editing, L.G.A., N.A.B.S.G. and A.E.R.; project administration, L.G.A. All authors have read and agreed to the published version of the manuscript.

Data Availability Statement: Not applicable.

Conflicts of Interest: The authors declare no conflict of interest.

References

1. Razzaq, R.; Shah, K.H.; Fahad, M.; Naeem, A.; Sherazi, T.A. Adsorption potential of macroporous Amberlyst-15 for Cd(II) removal from aqueous solutions Adsorption potential of macroporous Amberlyst-15 for Cd(II) removal from aqueous solutions. *Mater. Res. Express* **2020**, *7*, 025509. [CrossRef]
2. Ramírez, E.; Bringu, R.; Fit, C.; Tejero, J.; Cunill, F. Assessment of ion exchange resins as catalysts for the direct transformation of fructose into butyl levulinate. *Appl. Catal. A Gen.* **2021**, *612*, 117988. [CrossRef]
3. Silva, M.V.C.; Souza, A.B.; De Castro, H.F.; Aguiar, L.G.; De Oliveira, P.C.; De Freitas, L. Synthesis of 2-ethylhexyl oleate catalyzed by Candida antarctica lipase immobilized on a magnetic polymer support in continuous flow. *Bioprocess Biosyst. Eng.* **2020**, *43*, 615–623. [CrossRef] [PubMed]

4.   Aguiar, L.G.; Godoy, W.M.; Nápolis, L.; Faria, R.P.V.; Rodrigues, A.E. Modeling the Effect of Cross-Link Density on Resins Catalytic Activities. *Ind. Eng. Chem. Res.* **2021**, *60*, 6101–6110. [CrossRef]

5.   Pariente, S.; Tanchoux, N.; Fajula, F. Etherification of glycerol with ethanol over solid acid catalysts. *Green Chem.* **2009**, *11*, 1256–1261. [CrossRef]

6.   Jagadeeshbabu, P.E.; Sandesh, K.; Saidutta, M.B. Kinetics of esterification of acetic acid with methanol in the presence of ion exchange resin catalysts. *Ind. Eng. Chem. Res.* **2011**, *50*, 7155–7160. [CrossRef]

7.   Carpegiani, J.A.; Godoy, W.M.; Guimarães, D.H.P.; Aguiar, L.G. Glycerol acetylation catalyzed by an acidic styrene-co-dimethacrylate resin: Experiments and kinetic modeling. *React. Kinet. Mech. Catal.* **2020**, *130*, 447–461. [CrossRef]

8.   Güemez, M.B.; Requies, J.; Agirre, I.; Arias, P.L.; Barrio, V.L.; Cambra, J.F. Acetalization reaction between glycerol and n-butyraldehyde using an acidic ion exchange resin. Kinetic modelling. *Chem. Eng. J.* **2013**, *228*, 300–307. [CrossRef]

9.   Orjuela, A.; Yanez, A.J.; Santhanakrishnan, A.; Lira, C.T.; Miller, D.J. Kinetics of mixed succinic acid/acetic acid esterification with Amberlyst 70 ion exchange resin as catalyst. *Chem. Eng. J.* **2012**, *188*, 98–107. [CrossRef]

10. Edebali, S.; Pehlivan, E. Evaluation of Amberlite IRA96 and Dowex 1×8 ion-exchange resins for the removal of Cr(VI) from aqueous solution. *Chem. Eng. J.* **2010**, *161*, 161–166. [CrossRef]

11. Badia, J.H.; Fité, C.; Bringué, R.; Iborra, M.; Cunill, F. Catalytic Activity and Accessibility of Acidic Ion-Exchange Resins in Liquid Phase Etherification Reactions. *Top. Catal.* **2015**, *58*, 919–932. [CrossRef]

12. Van de Steene, E.; De Clercq, J.; Thybaut, J.W. Ion-exchange resin catalyzed transesterification of ethyl acetate with methanol: Gel versus macroporous resins. *Chem. Eng. J.* **2014**, *242*, 170–179. [CrossRef]

13. Chandane, V.S.; Rathod, A.P.; Wasewar, K.L.; Sonawane, S.S. Esterification of propionic acid with isopropyl alcohol over ion exchange resins: Optimization and kinetics. *Korean J. Chem. Eng.* **2017**, *34*, 249–258. [CrossRef]

14. Serrano, D.P.; Melero, J.A.; Morales, G.; Iglesias, J.; Pizarro, P. Progress in the design of zeolite catalysts for biomass conversion into biofuels and bio-based chemicals. *Catal. Rev.—Sci. Eng.* **2018**, *60*, 1–70. [CrossRef]

15. Mane, S.; Ponrathnam, S.; Chavan, N. Effect of Chemical Crosslinking on Properties of Polymer Microbeads: A Review. *Can. Chem. Trans.* **2016**, *3*, 473–485. [CrossRef]

16. Tejero, M.A.; Ramírez, E.; Fité, C.; Tejero, J.; Cunill, F. Esterification of levulinic acid with butanol over ion exchange resins. *Appl. Catal. A Gen.* **2016**, *517*, 56–66. [CrossRef]

17. Theodoro, T.R.; Dias, J.R.; Penariol, J.L.; Moura, J.O.V.; Aguiar, L.G. Sulfonated poly (styrene-co-ethylene glycol dimethacrylate) with attractive ion exchange capacity. *Polym. Adv. Technol.* **2018**, *29*, 2759–2765. [CrossRef]

18. Carpegiani, J.A. Study of Mathematical Modeling of Glycerol Acetylation with Different Catalysts. Master Thesis, Escola de Engenharia de Lorena, Universidade de São Paulo, Lorena, SP, Brazil, 2020.

19. Silva, V.F.L.; Penariol, J.L.; Dias, J.R.; Theodoro, T.R.; Carpegiani, J.A.; Aguiar, L.G. Sulfonated Styrene—Dimethacrylate Resins with Improved Catalytic Activity. *Kinet. Catal.* **2019**, *60*, 654–660. [CrossRef]

20. Kong, X.Z.; Gu, X.L.; Zhu, X.; Zhang, L. Precipitation polymerization in ethanol and ethanol/water to prepare uniform microspheres of poly(TMPTA-styrene). *Macromol. Rapid Commun.* **2009**, *30*, 909–914. [CrossRef]

21. Karam, H.J.; Tien, L.; Dour, T.; Company, C. Analysis of Swelling of Crosslinked Rubber Gel with Occlusions. *J. Appl. Polym. Sci.* **1988**, *30*, 1969–1988. [CrossRef]

22. Ho, L.-H.; Feng, S.-Y.; Yen, T.-M. A New Methodology for Customer Satisfaction Analysis: Taguchi's Signal-to-Noise Ratio Approach. *J. Serv. Sci. Manag.* **2014**, *07*, 235–244. [CrossRef]

23. Wolde-rufael, Y.; Idowu, S. Income distribution and CO_2 emission: A comparative analysis for China and India. *Renew. Sustain. Energy Rev.* **2017**, *74*, 1336–1345. [CrossRef]

24. Phadke, M.S.; Kackar, R.N.; Speeney, D.V.; Grieco, M.J. Off-line quality control in integrated circuit fabrication using experimental design. *Bell Syst. Tech. J.* **1983**, *62*, 1273–1309. [CrossRef]

25. Okay, O. Macroporous copolymer networks. *Prog. Polym. Sci.* **2000**, *25*, 711–779. [CrossRef]

26. Jerábek, K. Characterization of Swollen Polymer Gels Using Size Exclusion Chromatography. *Anal. Chem.* **1985**, *57*, 1598–1602. [CrossRef]

27. NanoComposix Molecular Weight to Size Calculator. Available online: https://nanocomposix.com/pages/molecular-weight-to-size-calculator (accessed on 18 October 2022).

28. Bringué, R.; Ramírez, E.; Tejero, J.; Cunill, F. Esteri fi cation of furfuryl alcohol to butyl levulinate over ion-exchange resins. *Fuel* **2019**, *257*, 116010. [CrossRef]

29. Faria Neto, A.; Costa, A.F.B.; de Lima, M.F. Use of Factorial Designs and the Response Surface Methodology to Optimize a Heat Staking Process. *Exp. Tech.* **2018**, *42*, 319–331. [CrossRef]

30. Godoy, W.M. Synthesis and Characterization of Polymerics Catalysts from Styrene Base, and Application in the Glycerol Acetylation. Master Thesis, University of São Paulo, Lorena, SP, Brazil, 2021.

31. Godoy, W.M.; Carpegiani, J.A.; Pereira, F.M.; Guimarães, D.H.P.; Aguiar, L.G. Kinetic modeling of glycerol acetylation catalyzed by styrene–divinylbenzene and styrene-trimethylolpropane triacrylate sulfonated resins. *React. Kinet. Mech. Catal.* **2022**, *135*, 233–245. [CrossRef]

32. Godoy, W.; Castro, G.; Nápolis, L.; Carpegiani, J.; Guimarães, D. Synthesis of Sulfonated Poly [Styrene-co-(Trimethylolpropane Triacrylate)] and Application in the Catalysis of Glycerol Acetylation. *Macromol. Symp.* **2020**, *394*, 1900169. [CrossRef]

33. Banu, I.; Bumbac, G.; Bombos, D.; Velea, S.; Gălan, A.-M.; Bozga, G. Glycerol acetylation with acetic acid over Purolite CT-275. Product yields and process kinetics. *Renew. Energy* **2020**, *148*, 548–557. [CrossRef]

34. Gomes, J.T.S.; Santos, J.H.S.; Abreu, C.A.M.; Medeiros, E.B.M.; Coelho, L.C.D.; Faria, R.P.V.; Rodrigues, A.E.; Lima Filho, N.M. Development and validation of analytical method for mono, di and triacetin analysis by HPLC/UV–Vis/DAD detection with 13C NMR identification. *Results Chem.* **2020**, *2*, 100063. [CrossRef]

35. Perez, F.M.; Gatti, M.N.; Nichio, N.N.; Pompeo, F. Results in Engineering Bio-additives from glycerol acetylation with acetic acid: Chemical equilibrium model. *Results Eng.* **2022**, *15*, 100502. [CrossRef]